

Article

Enhancing the Raveling Resistance of Polyurethane Mixture: From the Perspective of Polyurethane Adhesive

Junfeng Gao ^{1,2}, Hainian Wang ^{2,*}, Jiakang Chen ³ and Boming Tang ¹

- ¹ National & Local Joint Engineering Research Center of Transportation and Civil Engineering Materials, Chongqing Jiaotong University, Chongqing 400074, China
- ² Key Laboratory for Special Area Highway Engineering of Ministry of Education, Chang'an University, Xi'an 710064, China
- ³ Construction Management Branch of Shaanxi Transportation Holding Group Co., Ltd., Xi'an 710075, China
- * Correspondence: wanghn@chd.edu.cn

Abstract: Polyurethane mixture, made of waste rubber particle, aggregate, and polyurethane adhesive, has low raveling resistance which affects the durability of the mixture. The objective of this study is to enhance the raveling resistance of polyurethane mixture. The content of polyol in the hydroxyl component was determined by Fourier transform infrared spectroscopy. The suitable curing conditions for polyurethane adhesive to enhance the raveling resistance were selected by the orthogonal experiment and mechanical tests. The relationship of the raveling resistance with crosslink density and elastic modulus was tested and calculated through the wear test. The results showed that when the ratios of the isocyanate component to the hydroxyl component were 1:3.2, 1:6.3, and 1:9.5, respectively, the isocyanate component was excessive. The ranking of the significance of the influence factors, from high to low, was first the curing temperature, then curing time, and finally the blending ratio; within the ranges of blending ratio, curing temperature, and curing time selected in this study, the appropriate blending ratio was 10:2, and the curing time was 6 h. For the polyurethane mixture involved in this study to obtain high raveling resistance, if a crosslinking agent or a new polyurethane adhesive is added, the tensile strength and tensile elastic modulus should be in the range of 3.02 to 3.27 MPa and 5.50 to 6.02 MPa, respectively; when using the FS2 polyurethane adhesive directly, the suitable curing conditions for the mixture are 90 °C and 6 h or 80 °C and 6 h. The results from this study could be beneficial for obtaining a high raveling resistance for the polyurethane mixture.

Keywords: polyurethane adhesive; polyurethane mixture; curing condition; wear test; direct tensile test; raveling resistance



Citation: Gao, J.; Wang, H.; Chen, J.; Tang, B. Enhancing the Raveling Resistance of Polyurethane Mixture: From the Perspective of Polyurethane Adhesive. *Coatings* **2022**, *12*, 1950. <https://doi.org/10.3390/coatings12121950>

Academic Editor: Mariaenrica Frigione

Received: 31 October 2022

Accepted: 5 December 2022

Published: 12 December 2022

Publisher's Note: MDPI stays neutral with regard to jurisdictional claims in published maps and institutional affiliations.



Copyright: © 2022 by the authors. Licensee MDPI, Basel, Switzerland. This article is an open access article distributed under the terms and conditions of the Creative Commons Attribution (CC BY) license (<https://creativecommons.org/licenses/by/4.0/>).

1. Introduction

In recent years, the growing number of vehicles has led to tons of waste tires being generated in the world, which has brought a great challenge for the recycling of scrap tires [1–3]. The rubber, the main content of tire, is difficult to decompose completely, and it has a negative effect on the environment. Thus, researchers in the field of road engineering make efforts to seek environmentally friendly solutions for the utilization of waste rubber [4–7]. One of the main ways is to grind the tire rubber to powder and add it into the asphalt binder as an additive for improving road properties [8] while reducing the utilization of other polymer additives and raw materials [9–12]. Another main method is using the rubber particle as a kind of fine aggregate to partly replace the aggregate in asphalt mixtures and improve the deicing performance of asphalt mixtures [13–16]. The continuous seeking for ways to utilize tire rubber in road pavement enhances the development of poroelastic road surfaces. Poroelastic road surfaces are mainly composed of rubber particles processed from waste tires, some aggregates, and polyurethane adhesive [17]. They are mostly used in the surface of the pavement to reduce the tire–pavement noise due to its

high air void (up to 40%) and high elasticity [18], since a pavement with a high air void is a sustainable infrastructure tool used to benefit urban resilience [19].

The concept of poroelastic road surfaces was introduced in Sweden in the late 1970s. Later, some test tracks were paved in Japan [20,21]. In 2009, a project named PoroElastic Road Surface to Avoid Damage to the Environment (PERSUADE) in Europe was launched for testing the concept to reduce road noise [22,23]. The project proved that a poroelastic road surface could reduce noise by 10–12 dB [24,25]. Meanwhile, some performances, such as raveling resistance and durability, were found to be a challenge for the further utilization of poroelastic road surfaces in this project. Following this project, some researchers also conducted further study on the poroelastic road surface. Krishna et al. prepared five different poroelastic mixtures and characterized the fundamental material performances of these mixtures by the stress–strain test and dynamic modulus test. These indicated that the poroelastic mixture was softer than the conventional asphalt concrete, which plausibly provided a high noise-dampening response [26]. Jerzy et al. measured the tire–road noise and compared the rolling resistance of car tires on the poroelastic road surface and on conventional asphalt concrete [27]. Srirangam et al. explored the stress distribution on the poroelastic road surface under heavy loads using finite element simulations, and determined that the response of this layer is influenced by the stiffness of the adhesive layer [28]. Wang et al. evaluated the suitability of poroelastic road surfaces for urban roads in cold areas by testing their low-temperature cracking resistance, acoustic performance, and deicing performance [29]. Wang et al. also investigated the influences of different composition factors on the raveling resistance, and quantified the raveling resistance of PERS by measuring the material loss after polishing [17]. In addition, the chemical structures of polyurethane have also been changed and applied to other pavement practices, including as pavement repairing material, permeable pavement material, tunnel paving material and bridge deck paving material, ultra-thin friction course material, etc. [30,31].

The poroelastic road surface has prominent reduction of the noise generated by the tire–road. However, the raveling resistance found by the PERSUADE project is a limitation for the durability of its utilization, and it is barely studied. At the same time, the relationship between polyurethane mechanical indicators and the raveling resistance performance of polyurethane mixtures has not been studied. This study aims to enhance the raveling resistance using the curing conditions and tensile strength of polyurethane adhesive. The content of polyol in the hydroxyl component was determined by Fourier transform infrared (FTIR) spectroscopy [32,33]. The most suitable curing condition for polyurethane adhesive was selected through the orthogonal experiment and mechanical tests. The relationship of the raveling resistance with the crosslink density and elastic modulus was tested and calculated by the wear test.

2. Materials and Methods

2.1. Materials

In this study, a two-component solvent-free polyurethane adhesive was used based on the analysis of previous research; it was mainly composed of a hydroxyl component (A) and an isocyanate component (B). It was provided by a company, and part B was 4-4'-diphenylmethane diisocyanate (Figure 1), but the specific ingredients of part A were uncertain. The two components were blended according to a certain ratio and reacted to form a polyurethane adhesive. The type of polyurethane adhesive used in this study was FS2.

The rubber granule used in this study was made of waste rubber tire. The shape was cubic and the particle size was 4.75 mm. The aggregate used in this study was quartz sand, and its SiO₂ content was more than 95%. Its particle size was 1.18 mm, and the apparent density was 2.702 g·cm⁻³. To make the mixture have high air void, the contents of polyurethane adhesive were 30% by weight of the total mass of the mixture.

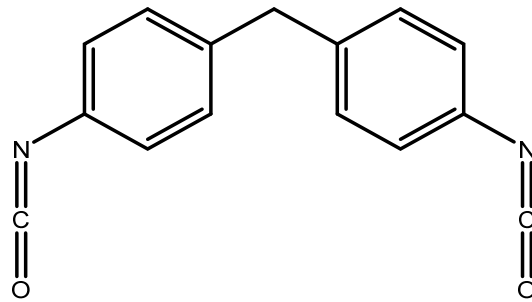


Figure 1. 4-4'-diphenylmethane diisocyanate.

2.2. Methods

2.2.1. Fourier Transform Infrared Spectroscopy Test

Fourier transform infrared spectroscopy test is a method to analyze the functional group of material. The instrument was a Bruker TENSOR 27. The scanning range was 4000–600 cm^{-1} , while the resolution was 0.4 cm^{-1} .

2.2.2. Direct Tensile Test

The direct tensile test of polyurethane adhesive was used to determine the tensile strength of the polyurethane adhesive, indirectly reflecting the adhesion between polyurethane and rubber granule. This test was conducted by universal testing machine (UTM). The samples were prepared according the specification test methods for properties of resin casting body (GB/T 2567-2008). Five replicates were set under the same regimen for each blending ratio. The temperature of the direct tensile test was 23 °C, and the tensile rate was 10 mm/min.

2.2.3. Crosslink Density Test

The crosslink density is an important index to evaluate the degree of crosslinking of the polymer material, and it is represented by the number of moles of crosslinking bonds per unit volume of the cross-linked polymer [34–36]. The higher the crosslink density, the better the thermal stability of the polymer material. In this study, the stress–strain curve obtained by UTM (the tensile rate was 2 mm/min) was used to calculate the crosslink density of the polyurethane adhesive. The tensile elastic modulus was first calculated from the linear segment of the stress and strain curve, and then the crosslink density was calculated based on Equation (1).

$$v_E = \frac{E_t}{3RT} \quad (1)$$

where E_t is tensile elastic modulus, MPa; v_E is crosslink density, mol/m^3 ; R is gas constant, 8.314 J/mol·K; and T is the absolute temperature at the time of testing, K.

2.2.4. Wear Test

The pavement accelerated wear instrument (shown in Figure 2), designed at Chang'an University, was used to simulate the mass loss process of polyurethane mixture under the repeated action of wheel load to characterize its raveling resistance. It consists of four parts: drive system, control system, water spray system, and frame. The tire is a polyurethane industrial tire with a hardness of 70–75 A, a tire pressure of 0.7 MPa, a diameter of 200 mm, and a width of 45 mm. The wear width with the specimen is increased to 90 mm by the layout of the tire. The tire running track is a circular ring, on which it is easy to accelerate wear, and the inner circle radius of the wear surface is 100 mm. The test was conducted at room temperature.

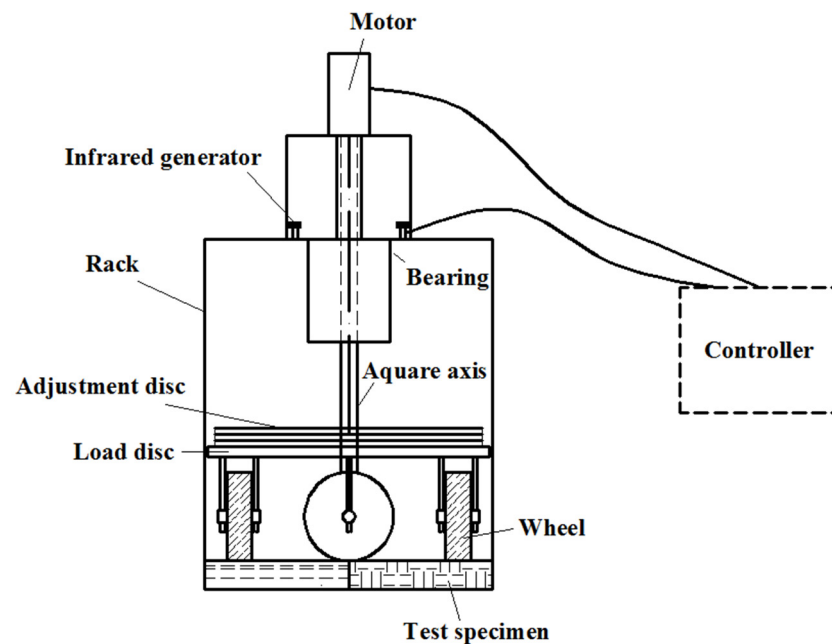


Figure 2. Wear test.

Based on the previous literature, the evaluation method for the raveling resistance in this study was proposed, that is, the height reduction value at the wear position. The greater the height reduction value, the lower the raveling resistance. It was calculated by Equation (2).

$$\Delta h = h_0 \times \frac{M_0 - M_t}{M_0 \times \frac{S_t}{S_0}} \quad (2)$$

where Δh is the height reduction value at the wear position after abrasion, mm; h_0 is the height at the wear position before abrasion, which is 50 mm; M_t is the mass of the specimen after abrasion, g; M_0 is the mass of the specimen before abrasion, g; S_t is the surface wear area of the specimen, calculated according to Equation (3), mm²; and S_0 is the surface area of the specimen, which is 300² mm².

$$S_t = \frac{[\pi(R + 90)^2 - \pi R^2]}{4} \quad (3)$$

where R is the inner radius of the wear area, 100 mm.

In this study, the accelerated wear instrument was used to perform 1000 r, 2000 r, 4000 r, 8000 r, and 16,000 r on the specimen, and the mass loss of the specimen was measured.

To analyze the different curing conditions of polyurethane adhesive on the raveling resistance of polyurethane mixture, the difference $\Delta(\Delta h)$ between the height decrease value Δh under a certain condition and that of the original curing condition (60 °C and 12 h) was proposed. The calculation is shown as Equation (4).

$$\Delta(\Delta h_n) = \Delta h_{0n} - \Delta h_n \quad (4)$$

where $\Delta(\Delta h_n)$ is the difference between the height decrease value under a certain condition and that of the original curing condition (60 °C and 12 h), when the abrasion number is n , mm; Δh_{0n} is the height decrease value of specimen cured under the condition of 60 °C and 12 h, when the abrasion number is n , mm; Δh_n is the height decrease value of specimen cured under a certain condition, when the abrasion number is n , mm.

It can be known from Equation (4) that if the value of the $\Delta(\Delta h)$ of the specimen is higher than zero under a certain condition, the raveling resistance of the polyurethane

mixture is improved under the condition. The larger the value of $\Delta(\Delta h)$, the higher the raveling resistance of the polyurethane mixture under this condition.

2.2.5. Samples Preparation

For the direct tensile test, the samples of polyurethane adhesive were prepared by mixing the hydroxyl component (A) and isocyanate component (B) with the mixer and curing at different conditions. For the wear test, the slab specimens were prepared as follows: the polyurethane adhesive, rubber granules, and aggregates were first mixed; the mixed polyurethane mixture was loaded into the slab specimen forming device; and then the mold with mixture was placed on the wheel rolling forming instrument for compaction, as shown in Figure 3. A total of 24 cycles of compaction were conducted. After the compaction of the specimen, the top cover was covered, and the mixture was cured at 60 °C for 12 h.



Figure 3. Rolling process of the mixture.

2.2.6. Orthogonal Experimental Design

To make the excess isocyanate form a cross-linking under appropriate curing conditions and increase the tensile strength of the polyurethane adhesive, three different factors and three different levels were selected, and the orthogonal experimental design was proposed. The factors were the blending ratio of the hydroxyl component to the isocyanate component (factor A), the curing temperature of polyurethane adhesive (factor B), and the curing time (factor C). The specific influencing factors and levels are shown in Table 1.

Table 1. The various factors and levels for the polyurethane adhesive.

Factor	Level		
	1	2	3
Blending ratio A	10:2 (5:1)	10:2.5 (4:1)	10:3
Curing temperature B (°C)	60	80	100
Curing time C (h)	4	6	8

3. Results and Discussion

3.1. Determination of Polyol and Its Portion

The hydroxyl component (A) consists of polyol and some additives, such as catalyst and filler. In this section, the polyol and its portion were determined.

3.1.1. Preliminary Determination of Hydroxyl Component

The component A of FS2 polyurethane adhesive was a milky white and viscous liquid at room temperature. Component A could be isolated and a yellow liquid could

be separated on the surface if it was stored for a long time. Therefore, the yellow liquid was extracted before the determination of component A. The details of the extraction are as follows.

A total of 150 g of component A was placed in a 300 mL centrifuge tube, and 80 g of a colorless organic solvent, ethyl acetate, was added into the centrifuge tube and stirred. The viscous component A was completely dissolved in ethyl acetate, and the weight of each of the four centrifuge tubes centrifuged was 290 g. The centrifuge speed was set as 5000 r/min, the four centrifuge tubes in the centrifuge were centrifuged for 10 min, and the centrifuge tube was taken out after the centrifuge stopped running. The original liquid in the centrifuge tube was separated into an upper yellow liquid and a lower white viscous solid.

The yellow liquid in the centrifuge tube was collected, and it contained both the original yellow liquid of component A and the organic solvent ethyl acetate. Then, it was separated by distillation. The collected 200 mL of yellow liquid was poured into a 500 mL round bottom flask, and the round bottom flask was connected to a buffer and mounted on a rotary evaporator. The water bath temperature was 60 °C, the air pressure was 127 hPa, and the rotary evaporation was about 25 min until there was no more liquid condensation on the surface of the condenser. The organic solvent ethyl acetate in the round bottom flask was extracted, and the remaining liquid was the original yellow liquid in component A.

A total of 20 g of the original yellow liquid in component A was poured into the beaker, an equal mass of polyethylene glycol was added into the beaker according to the ratio of 1:1, they were stirred evenly at room temperature, and the mixture in the beaker could not cure within 72 h. In the same way, 20 g of component B (MDI) and 20 g of the original yellow liquid of component A were added into the beaker and stirred to obtain a yellow–brown liquid. During the stirring process, the two reacted, and the viscosity of the liquid in the beaker was continuously increased. The yellow–brown liquid lost fluidity and solidified to a yellow–brown solid two hours later. The solidified material in the beaker was placed in a 60 °C oven and the solid in the beaker was not found to change, indicating that component B reacted with the yellow liquid in component A to form a new substance.

When the white viscous solid remaining in the centrifuge tube was set at room temperature for 5 days, most of the residual organic solvent ethyl acetate had volatilized, thereby becoming a white powdery solid. A total of 20 g of the white powdery solid was placed in a beaker, and 40 g of component A was poured in for a ratio of 1:2 and stirred. After stirring evenly, the white powder was suspended in the isocyanate component, and the curing reaction of the mixture in the beaker could not be observed after 72 h.

To analyze the percentage of the yellow liquid reacting with component A, the above dissolution and centrifugation was repeated; the test results are shown in Table 2. The mass percentage of the yellow liquid was 31.58% after taking the average of the four test results.

Table 2. Percentage of yellow liquid mass in component A.

NO.	Mass of Centrifuge Tube (g)	Mass of Component A (g)	Total Mass after Centrifugation (g)	Percentage (%)
1	68.2	99.9	135.6	32.53
2	62.7	98.9	130.7	31.24
3	67.1	99.9	136.5	30.53
4	67.2	99.9	135.1	32.03

Note: Total mass after centrifugation was the mass of the centrifuge tube, the mass of the white powder solids, and the total mass of the residual organic solvent.

Component A of the FS2 type polyurethane adhesive was a hydroxyl component, which contained a yellow liquid capable of reacting with isocyanate, and a white powdery solid which did not participate in the reaction. The yellow liquid percentage in component A was 31.58%. The yellow liquid contained a polyol capable of reacting with isocyanate, so the yellow liquid was named as a polyol liquid, and the white powdery solid was a solid

filler in the hydroxyl component and an auxiliary agent. The infrared spectroscopy of the polyol liquid is shown in Figure 4.

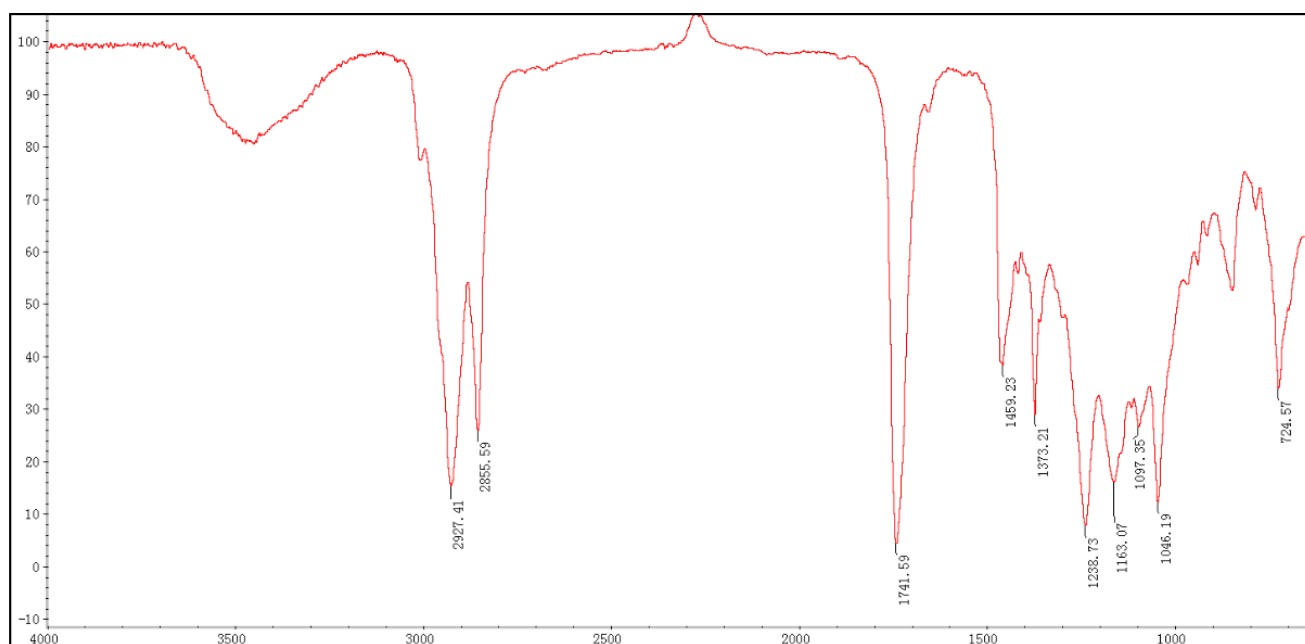


Figure 4. The infrared spectroscopy of the polyol liquid.

It can be seen from Figure 4 that three absorption peaks were more obvious, and the wave numbers were 2929.41 cm^{-1} , 2855.59 cm^{-1} , and 1741.59 cm^{-1} , respectively. The two absorption peaks with wave numbers of 2927.41 cm^{-1} and 2855.59 cm^{-1} correspond to methylene ($-\text{CH}_2-$), and the absorption peak with the wave number of 1741.95 cm^{-1} corresponds to ester group ($\text{C}=\text{O}$). Therefore, it can be inferred from the figure that the polyol may contain more ester groups, that is, it may be a polyester polyol. In addition, there were many peaks at $1000\text{--}1300\text{ cm}^{-1}$ in the spectrum, and the $\text{C}-\text{O}$ bonds of ether, ester, alcohol and other functional groups all have peaks in this range, so the material structure cannot be estimated as a characteristic peak [37,38]. Therefore, it was difficult to analyze the molecular structure of the polyester polyol by infrared spectroscopy or other methods. Since the molecular structure of the polyol was not involved in the subsequent studies, no further analysis was performed here.

3.1.2. The Blending Ratio of Hydroxyl Component (A) and an Isocyanate Component (B)

The isocyanate component (B) and the polyol liquid of hydroxyl component (A) were placed in a wide-mouth bottle at a ratio of 1:1, 1:2, and 1:3, respectively, and stirred for 72 h. After the two fully reacted, a small amount of the material in the wide-mouth bottle was taken for infrared spectrum analysis, and the results are shown in Figure 5.

The isocyanate group absorption peak wave number was $2240\text{--}2280/\text{cm}^{-1}$. As shown in Figure 5, when the blending ratios of the isocyanate component and the polyol liquid were 1:1, 1:2, and 1:3, the absorption peak of the isocyanate group existed, and the wave numbers were 2259.86 cm^{-1} , 2273.10 cm^{-1} , and 2276.64 cm^{-1} , respectively. However, the peak intensity of the isocyanate group decreased as the amount of polyol liquid was increased.

It can be found that when the blending ratios of the isocyanate component to the polyol liquid were 1:1, 1:2, or 1:3, the isocyanate component was excessive, so that after the reaction for 72 h, some of the isocyanate MDI was still not involved in the reaction. The polyol liquid accounted for about 31.58% of the hydroxyl component (A); therefore, when the ratios of the isocyanate component to the hydroxyl component (A) were 1:3.2, 1:6.3, and 1:9.5, respectively, the isocyanate component was excessive. Therefore, to ensure the

forming of cross-linking under the condition of the excessive isocyanate component, three ratios, 3:10, 2.5:10, and 2:10, were selected for the further test.

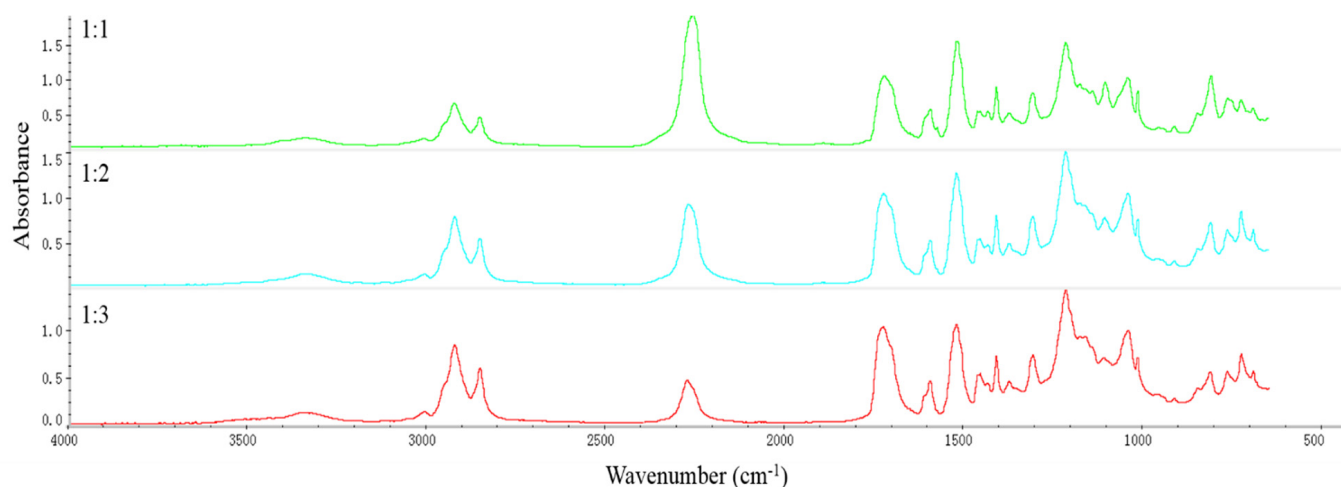


Figure 5. Infrared analysis results after reaction of isocyanate component and polyol liquid.

3.2. Results of the Orthogonal Experiment

Due to the significant relationship between tensile strength and the blending ratio (factor A), curing temperature (factor B), and curing time (factor C) of polyurethane adhesive, a three-factor, three-level orthogonal test was conducted to analyze the significance of the influence of the three factors on the tensile strength of polyurethane adhesive. The test results are shown in Table 3.

Table 3. Orthogonal test results for tensile strength and various factors of polyurethane adhesive.

No.	Blending Factor A	Curing Temperature B (°C)	Curing Time C (h)	Tensile Strength (MPa)
1	10:2	60	4	2.37
2	10:2	80	6	3.02
3	10:2	100	8	3.81
4	10:2.5	60	6	2.11
5	10:2.5	80	8	2.54
6	10:2.5	100	4	2.60
7	10:3	60	8	1.45
8	10:3	80	4	1.60
9	10:3	100	4	4.68

The curing conditions recommended by the manufacturer of FS2 polyurethane adhesive were 6 h at 60 °C, and the curing conditions of the previous polyurethane mixture were 12 h at 60 °C. Therefore, the tensile strengths of the polyurethane adhesive under these two conditions were 2.62 MPa and 2.69 MPa, respectively.

As shown in Table 4, the tensile strength of polyurethane adhesive was affected by the blending ratio of the isocyanate component and the hydroxyl component, the curing temperature, and the curing time. The results of experiments 1 to 3 in Table 2 show that the tensile strength of the polyurethane adhesive was significantly enhanced after increasing the curing temperature and increasing the curing time; especially, the test results of experiment 2 and experiment 3 were significantly higher than 60 °C and 6 h. The results of experiments 4, 5, 7, and 8 show that when the curing temperature was lower than 100 °C, increasing the amount of isocyanate lowered the tensile strength. However, from the results of experiments 6 and 9, it was known that the tensile strength of the polyurethane adhesive was remarkably improved when the curing temperature was 100 °C. Therefore, when the isocyanate was excessive in the polyurethane adhesive, an increase in the curing temperature and the curing time could increase the tensile strength

of the polyurethane adhesive; however, when the isocyanate component was added in a higher amount, the tensile strength of the polyurethane adhesive could be improved only at a higher curing temperature.

Table 4. Mean and range of tensile strength for each factor at each level (unit: MPa).

Level \ Factor		A	B	C
		1	3.067	1.977
2		2.417	2.387	3.267
3		2.573	3.693	2.600
Sample range		0.650	1.716	0.836

Note: A—blending ratio, B—curing temperature, C—curing time; the meanings of levels 1, 2, and 3 are shown in Table 1.

It can be seen in Table 4 that there was a significant difference in the influence of the blending ratio of the polyurethane adhesive, the curing temperature, and the curing time on the tensile strength of the polyurethane adhesive. According to the range of values, the significance ranking of the influence from high to low was, first, the curing temperature, then the curing time, and finally the blending ratio. The mean of the tensile strength of factor A at level 1 was the maximum among the levels within factor A, while the mean of the tensile strength of factor C at level 2 was the maximum among the levels within factor C. Therefore, the appropriate blending ratio in this study was 10:2, and the curing time was 6 h.

To further analyze the influence rule of curing temperature on the tensile strength of the polyurethane adhesive, the tensile strength was tested with a blending ratio of 10:2, a curing time of 6 h, and curing temperatures of 70 °C, 90 °C, and 100 °C. The tensile strengths tested at the three curing temperatures were 2.83 MPa, 3.27 MPa, and 3.61 MPa, respectively. This indicated that when the blending ratio and the curing time were constant, the tensile strength of the polyurethane adhesive increased as the curing temperature increased.

Different tensile strengths and elongations at break under different conditions were selected for further analysis, as shown in Table 5.

Table 5. Different tensile strengths and elongations at break under different conditions.

No.	Blending Ratio	Curing Temperature (°C)	Curing Time (h)	Tensile Strength (MPa)	Elongation at Break (%)
1	10:2	60	12	2.69	56.4
2	10:2	70	6	2.83	60.0
3	10:2	80	6	3.02	58.0
4	10:2	90	6	3.27	50.8
5	10:2	100	6	3.61	51.9
6	10:2	100	8	3.81	35.1

3.3. Crosslink Density and Elastic Modulus

The load–deformation diagrams for polyurethane adhesive under different curing conditions are shown in Figure 6.

As shown in Figure 6, when the specimen was stretched at a rate of 2 mm/min, the load on the specimen increased with a small fluctuation as the deformation increased, indicating that a small degree of relaxation occurred in the polyurethane adhesive during the tensile process. For the specimens cured under the conditions of 60 °C and 12 h and 70 °C and 6 h, the overall increase trend was approximately a straight line. Meanwhile, for the specimens cured under the conditions of 80 °C and 6 h, 90 °C and 6 h, 100 °C and 6 h, and 100 °C and 8 h, the load first increased with an approximately straight line as the displacement increased, and then the increasing trend gradually slowed down until the specimen broke. Therefore, the approximately straight line segment was fitted by the first polynomial $Y = A + BX$, and the straight line segment obtained by the fitting was regarded

as the initial straight line segment of the load–deformation; thereby, the elastic modulus of the polyurethane adhesive was calculated. The crosslink density was also obtained based on Equation (1).

It can be seen from Table 6 that the crosslink density and elastic modulus increased with an increase in curing temperature. This was because the excess MDI acted as a cross linker at higher temperatures, promoting the mutual crosslinking of the polyurethane binder molecules. Meanwhile, it can also be seen from Table 5 that the tensile strength also increased as the curing temperature increased. This was consistent with the previous study [39].

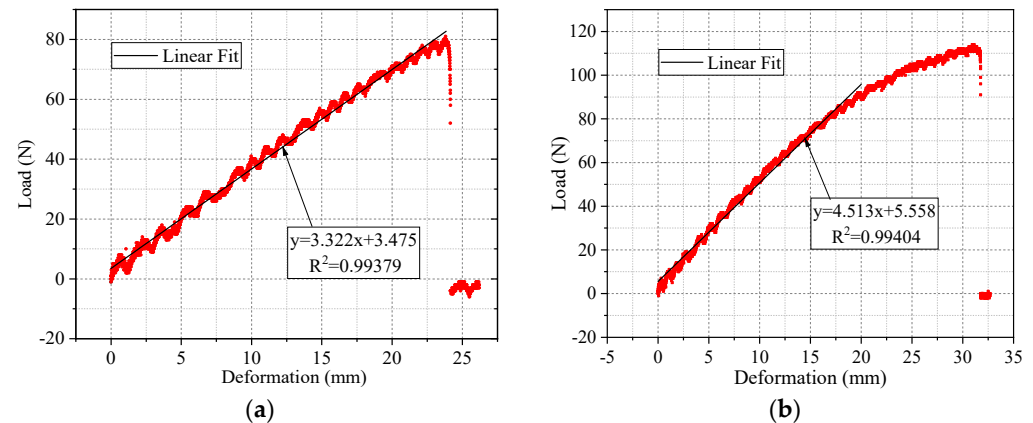


Figure 6. The relationship between tensile load and deformation of polyurethane under different curing conditions. (a) 60 °C & 12 h; (b) 90 °C & 6 h.

Table 6. Different elastic modulus and crosslink density under different conditions.

No	Blending Ratio	Curing Temperature (°C)	Curing Time (h)	Elastic Modulus (MPa)	Crosslink Density (mol·m ⁻³)
1	10:2	60	12	4.58	620.36
2	10:2	70	6	5.57	754.45
3	10:2	80	6	5.50	745.97
4	10:2	90	6	6.02	815.41
5	10:2	100	6	8.08	1094.43
6	10:2	100	8	9.07	1228.53

3.4. The Relationship between Raveling Resistance and Curing Conditions and Tensile Strength

3.4.1. Curing Conditions

To analyze the influence of the curing conditions on the raveling resistance, the decrease in the height Δh at the wear position was selected and fitted by the quadratic polynomial $Y = A + Bx + Cx^2$, and the relevant parameters obtained by fitting are shown in Table 7.

Table 7. Parameters of Δh quadratic polynomial fitting.

Curing Condition		60 °C & 12 h	70 °C & 6 h	80 °C & 6 h	90 °C & 6 h	100 °C & 6 h	100 °C & 8 h
Parameters	A	0.03528	−0.01467	−0.00297	−0.00206	−0.02537	0.03773
	B	0.12414	0.05188	0.04036	0.03515	0.04987	0.07204
	C	−0.00371	−0.00016	−0.00041	−0.00013	−0.00012	−0.00167
	R ²	0.98656	0.99836	0.99892	0.99635	0.98735	0.99204

It can be seen from Table 7 and Figure 7 that the Δh of the sled specimen increased with the increase in the number of abrasions, but the increasing trend gradually slowed down. At the same time, when the number of abrasions was the same, compared to the

decreasing height of polyurethane cured at the condition of 60 °C and 12 h, other decreases in height under different conditions were lower; Δh under the conditions of 80 °C and 6 h and 90 °C and 6 h was lowest. This meant that the change of curing condition improved the raveling resistance of the polyurethane mixture.

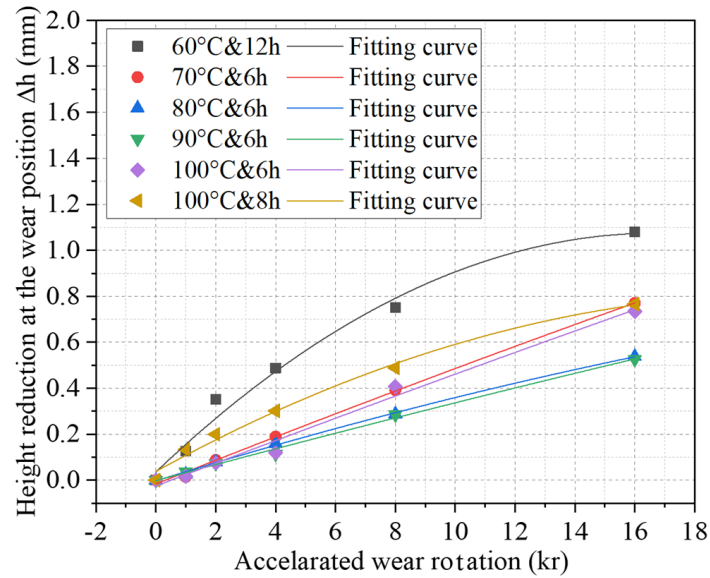


Figure 7. Δh fitting curve under different curing conditions.

3.4.2. Tensile Strength

The difference $\Delta(\Delta h)$ of polyurethane mixture under different conditions is shown in Figure 8. It can be seen from Figure 8 that the $\Delta(\Delta h)$ value of the specimens under 100 °C and 8 h after the wear of 1000 cycles was less than zero, and the $\Delta(\Delta h)$ values of other specimens after wear were higher than zero. Moreover, the tensile strength of the polyurethane adhesive under the original mixing condition (60 °C and 12 h) was 2.69 MPa, indicating that the increase in tensile strength of polyurethane adhesive can improve the raveling resistance of polyurethane mixture.

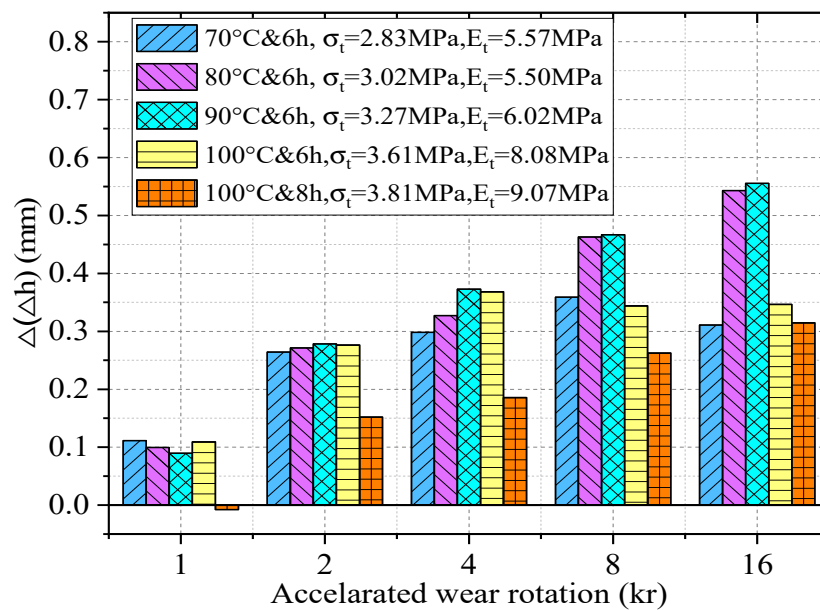


Figure 8. The difference $\Delta(\Delta h)$ of polyurethane mixture under different conditions.

At the same time, by comparing the $\Delta(\Delta h)$ of different specimens under the same wear number, it can be found that the mixture under the condition of 100 °C and 8 h had the lowest raveling resistance. The $\Delta(\Delta h)$ showed a significant difference when other specimens had a wear number of more than 4000 cycles. This indicated that the polyurethane mixture prepared under the conditions of 80 °C and 6 h and 90 °C and 6 h had higher raveling resistance, while the polyurethane mixtures prepared under the conditions of 70 °C and 6 h and 100 °C and 6 h were relatively low.

3.4.3. Specimens after Abrasion

It can be seen from Figure 9 that when the tensile strength of the polyurethane adhesive was 3.27 MPa, the raveling resistance of the mixture was the highest. When the tensile strength was 3.02 MPa, the raveling resistance of the mixture was high. When the tensile strength of the adhesive was less than 3.02 MPa, or more than 3.27 MPa, the raveling resistance of the mixture was relatively low at a higher wear number. When the wear number was 16,000 cycles, the specimens cured at the conditions of 70 °C and 6 h and 100 °C and 6 h had more solid particles peeled off from the surface than those of 80 °C and 6 h and 90 °C and 6 h.

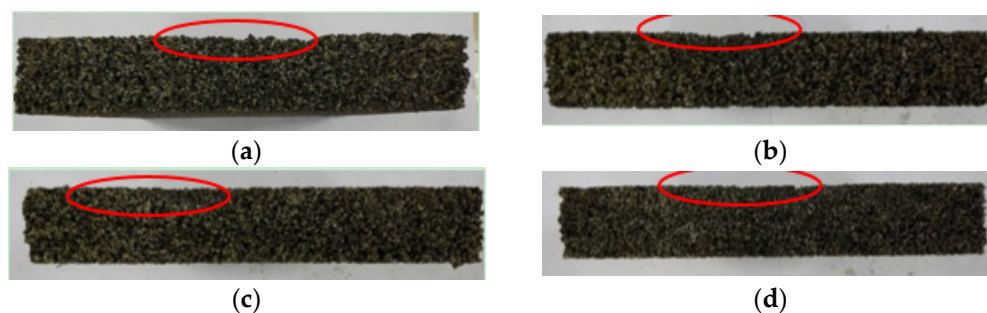


Figure 9. The side views of abrasion specimens under different curing conditions. (a) 70 °C & 6 h, Note: $\sigma = 2.83$ MPa, $E = 5.07$ MPa; (b) 100 °C & 6 h, Note: $\sigma = 3.61$ MPa, $E = 8.08$ MPa; (c) 90 °C & 6 h. Note: $\sigma = 3.27$ MPa, $E = 6.02$ MPa; (d) 80 °C & 6 h, Note: $\sigma = 3.02$ MPa, $E = 5.50$ MPa.

In a certain range, the increase in the tensile strength of polyurethane adhesive could improve the raveling resistance of the mixture to a certain extent, but beyond this range, the increase in tensile strength cannot improve its resistance. In addition, the increase in tensile strength depends on the increase in mutual crosslinking. However, this method of increasing the tensile strength of polyurethane adhesives obtained by increasing the degree of crosslinking also leads to a significant increase in the tensile modulus of polyurethane adhesives. Excessive tensile elastic modulus made the deformability of the polyurethane adhesive worse. Therefore, under the action of wheel load, the polyurethane adhesive was difficult to adapt to the uncoordinated deformation between the rubber particles and the fine aggregate, and the stress in the polyurethane adhesive exceeded the strength value prematurely.

It can be seen that to ensure the high raveling resistance of the polyurethane mixture, the tensile strength of the polyurethane adhesive should not be too low without changing the composition of the material of the mixture. At the same time, the tensile modulus should not be too high. For the polyurethane mixture involved in this study to have a high raveling resistance, if a crosslinking agent or a new polyurethane adhesive is added, the tensile strength and tensile elastic modulus should be in the range of 3.02 to 3.27 MPa and 5.50 to 6.02 MPa, respectively. When using FS2 polyurethane adhesive directly, the suitable curing conditions for the mixture are 90 °C and 6 h or 80 °C and 6 h.

4. Conclusions

This study investigated the methods to enhance the raveling resistance of polyurethane mixture from the perspective of polyurethane adhesive. The hydroxyl component was studied by the Fourier transform infrared spectroscopy. The curing condition of polyurethane adhesive was determined through the orthogonal experiment and mechanical tests. The ranges of tensile strength and tensile elastic modulus needed to have a high raveling resistance of polyurethane were proposed. The following conclusions are drawn.

- (1). The mass percentage in the polyol liquid was 31.58% for the hydroxyl component. When the ratios of the isocyanate component to the hydroxyl component were 1:3.2, 1:6.3, and 1:9.5, the isocyanate component was excessive. It was helpful to improve the crosslink density and the tensile strength.
- (2). The ranking of the significance of the influence factors, from high to low, was first the curing temperature, then the curing time, and finally the blending ratio; within the ranges of the blending ratio, curing temperature, and curing time selected in this experiment, the appropriate blending ratio was 10:2, and the curing time was 6 h.
- (3). For the polyurethane mixture involved in this study to have a high raveling resistance, if a crosslinking agent or a new polyurethane adhesive is added, the tensile strength and tensile elastic modulus should be in the range of 3.02 to 3.27 MPa and 5.50 to 6.02 MPa, respectively; when using FS2 polyurethane adhesive directly, the suitable curing conditions for the mixture are 90 °C and 6 h or 80 °C and 6 h.

Author Contributions: Conceptualization, H.W. and B.T.; materials and methods, J.G. and J.C.; experiments, J.G. and J.C.; writing—original draft preparation, J.G.; writing—review and editing, H.W.; supervision, H.W. and B.T. All authors have read and agreed to the published version of the manuscript.

Funding: This research was partially funded by the National Natural Science Foundation of China (NSFC) (Grant No. 52108399), Natural Science Foundation of Chongqing (Grant No. CSTB2022NSCQ-MSX0851), the Fundamental Research Funds for the Central Universities, CHD (Grant No. 300122 0221 2507), and China Postdoctoral Science Foundation (Grant No. 2022M710545).

Conflicts of Interest: The authors declare no conflict of interest.

References

1. Li, F.; Zhang, X.; Wang, L.; Zhai, R. The preparation process, service performances and interaction mechanisms of crumb rubber modified asphalt (CRMA) by wet process: A comprehensive review. *Constr. Build. Mater.* **2022**, *354*, 129168. [[CrossRef](#)]
2. Li, J.; Xiao, F.; Amirhanian, S. Storage, fatigue and low temperature characteristics of plasma treated rubberized binders. *Constr. Build. Mater.* **2019**, *209*, 454–462. [[CrossRef](#)]
3. Chen, Z.; Wang, T.; Pei, J.; Amirhanian, S.; Xiao, F.; Ye, Q.; Fan, Z. Low Temperature and Fatigue Characteristics of Treated Crumb Rubber Modified Asphalt after a Long Term Aging Procedure. *J. Clean Prod.* **2019**, *234*, 1262–1274. [[CrossRef](#)]
4. Sebaaly, P.E.; Gopal, V.T.; Epps, J.A. Low Temperature Properties of Crumb Rubber Modified Binders. *Road Mater. Pavement Des.* **2011**, *4*, 29–49. [[CrossRef](#)]
5. Xu, H.; McIntyre, A.; Adhikari, T.; Hesp, S.; Marks, P.; Tabib, S. Quality and Durability of Warm Rubberized Asphalt Cement in Ontario, Canada. *Transp. Res. Rec. J. Transp. Res. Board* **2013**, *2370*, 26–32. [[CrossRef](#)]
6. Liu, Q.; Liu, J.; Yu, B.; Zhang, J.; Pei, J. Evaluation and optimization of asphalt binder and mixture modified with high activated crumb rubber content. *Constr. Build. Mater.* **2022**, *314*, 125676. [[CrossRef](#)]
7. Attia, M. Enhancing the performance of crumb rubber-modified binders through varying the interaction conditions. *Int. J. Pavement Eng.* **2009**, *10*, 423–434. [[CrossRef](#)]
8. Gong, Z.; Zhang, L.; Wu, J.; Xiu, Z.; Wang, L.; Miao, Y. Review of regulation techniques of asphalt pavement high temperature for climate change adaptation. *J. Infrastruct. Preserv. Resil.* **2022**, *3*, 9. [[CrossRef](#)]
9. Lei, Y.; Wang, H.; Fini, E.H.; You, Z.; Yang, X.; Gao, J.; Dong, S.; Jiang, G. Evaluation of the effect of bio-oil on the high-temperature performance of rubber modified asphalt. *Constr. Build. Mater.* **2018**, *191*, 692–701. [[CrossRef](#)]
10. Liu, H.Y.; Chen, Z.J.; Wang, W.; Wang, H.N.; Hao, P.W. Investigation of the rheological modification mechanism of crumb rubber modified asphalt (CRMA) containing TOR additive. *Constr. Build. Mater.* **2014**, *67*, 225–233. [[CrossRef](#)]
11. Wang, H.; Dang, Z.; Li, L.; You, Z. Analysis on fatigue crack growth laws for crumb rubber modified (CRM) asphalt mixture. *Constr. Build. Mater.* **2013**, *47*, 1342–1349. [[CrossRef](#)]
12. Wang, H.N.; Zhang, C.; Li, L.; You, Z.P.; Diab, A. Characterization of Low Temperature Crack Resistance of Crumb Rubber Modified Asphalt Mixtures Using Semi-Circular Bending Tests. *J. Test. Eval.* **2016**, *44*, 847–855. [[CrossRef](#)]

13. Cao, D.W.; Zhang, Y.J.; Xia, L.; Li, Y.F.; Zhang, H.Y. Study on the Properties of Waterborne Polyurethane Modified Emulsified Asphalt. In Proceedings of the Transportation Research Congress 2016 (TRC), Beijing, China, 6–8 June 2016; pp. 207–215.
14. Chen, B.; Dong, F.Q.; Yu, X.; Zheng, C.J. Evaluation of Properties and Micro-Characteristics of Waste Polyurethane/Styrene-Butadiene-Styrene Composite Modified Asphalt. *Polymers* **2021**, *13*, 2249. [[CrossRef](#)] [[PubMed](#)]
15. Jin, X.; Guo, N.S.; You, Z.P.; Wang, L.; Wen, Y.K.; Tan, Y.Q. Rheological properties and micro-characteristics of polyurethane composite modified asphalt. *Constr. Build. Mater.* **2020**, *234*, 16. [[CrossRef](#)]
16. Yu, R.E.; Zhu, X.J.; Zhou, X.; Kou, Y.F.; Zhang, M.R.; Fang, C.Q. Rheological properties and storage stability of asphalt modified with nanoscale polyurethane emulsion. *Pet. Sci. Technol.* **2018**, *36*, 85–90. [[CrossRef](#)]
17. Wang, D.; Schacht, A.; Leng, Z.; Leng, C.; Kollmann, J.; Oeser, M. Effects of material composition on mechanical and acoustic performance of poroelastic road surface (PERS). *Constr. Build. Mater.* **2017**, *135*, 352–360. [[CrossRef](#)]
18. Sandberg, U.; Gubert, L. Poroelastic road surface (PERS): A review of 30 Years of R and D work. In Proceedings of the Inter-Noise and Noise-Con Congress and Conference Proceedings, InterNoise11, Osaka, Japan, 4–7 September 2011; pp. 3014–3021.
19. Zhang, K.; Kevern, J. Review of porous asphalt pavements in cold regions: The state of practice and case study repository in design, construction, and maintenance. *J. Infrastruct. Preserv. Resil.* **2021**, *2*, 4. [[CrossRef](#)]
20. Luc, G.; Ulf, S. PERSUADE Final Technical Report. In Proceedings of the Seventh framework programme of the European Community, Brussels, Belgium, 7 January 2016.
21. Kazuyuki, K. Present Status of Porous Elastic Rubber Surface (PERS) in Japan. In Proceedings of the Inter-Noise and Noise-Con Congress and Conference Proceedings, InterNoise11, Osaka, Japan, 4–7 September 2011; pp. 3147–3153.
22. Ulf, S.; Luc, G. PERSUADE—A European project for exceptional noise reduction by means of poroelastic road surfaces. In Proceedings of the Inter-Noise and Noise-Con Congress and Conference Proceedings, InterNoise11a, Osaka, Japan, 4–7 September 2011; pp. 2979–2989.
23. Goubert, L.; Sandberg, U.; Biligiri, K.P. State-of-the-Art Regarding Poroelastic Road Surfaces. In Proceedings of the Transportation Research Board (TRB) 89th Annual Meeting, Washington, DC, USA, 10–14 January 2020; p. 152.
24. Sandberg, U.; Kalman, B. The poroelastic road surface results of an experiment in Stockholm. In Proceedings of the Forum Acusticum: 4th European Congress on Acoustics, Budapest, Hungary, 29 August–2 September 2005; pp. 834–840.
25. Hitoshi, F.; Yoshifumi, A.; Kouji, H. Performance of the Porous Elastic Road Surface (PERS) as Low Noise Pavement. In Proceedings of the Inter-Noise and Noise-Con Congress and Conference Proceedings, InterNoise11, Osaka, Japan, 4–7 September 2011; pp. 2960–2966.
26. Biligiri, K.P.; Kalman, B.; Samuelsson, A. Understanding the fundamental material properties of low-noise poroelastic road surfaces. *Int. J. Pavement Eng.* **2013**, *14*, 12–23. [[CrossRef](#)]
27. Ejsmont, J.; Goubert, L.; Ronowski, G.; Świczko-Żurek, B. Ultra Low Noise Poroelastic Road Surfaces. *Coatings* **2016**, *6*, 18. [[CrossRef](#)]
28. Srirangam, S.K.; Anupam, K.; Casey, D.; Liu, X.; Kasbergen, C.; Scarpas, A. Evaluation of Structural Performance of Poroelastic Road Surfacing Pavement Subjected to Rolling-Truck Tire Loads. *Transp. Res. Rec. J. Transp. Res. Board* **2016**, *2591*, 42–56. [[CrossRef](#)]
29. Wang, D.; Liu, P.; Leng, Z.; Leng, C.; Lu, G.; Buch, M.; Oeser, M. Suitability of PoroElastic Road Surface (PERS) for urban roads in cold regions: Mechanical and functional performance assessment. *J. Clean Prod.* **2017**, *165*, 1340–1350. [[CrossRef](#)]
30. Hong, B.; Lu, G.; Li, T.; Lin, J.; Wang, D.; Liang, D.; Oeser, M. Gene-editable materials for future transportation infrastructure: A review for polyurethane-based pavement. *J. Infrastruct. Preserv. Resil.* **2021**, *2*, 27. [[CrossRef](#)]
31. Hong, B.; Lu, G.; Gao, J.; Dong, S.; Wang, D. Green tunnel pavement: Polyurethane ultra-thin friction course and its performance characterization. *J. Clean. Prod.* **2021**, *289*, 125131. [[CrossRef](#)]
32. Mohammad Asib, A.S.; Rahman, R.; Romero, P.; Hoepfner, M.P.; Mamun, A. Physicochemical characterization of short and long-term aged asphalt mixtures for low-temperature performance. *Constr. Build. Mater.* **2022**, *319*, 126038. [[CrossRef](#)]
33. Zhang, H.; Duan, H.; Luo, H.; Shi, C. Synthesis, characterization and utilization of zinc oxide/expanded vermiculite composite for bitumen modification. *Fuel* **2021**, *306*, 121731. [[CrossRef](#)]
34. Sekkar, V.; Narayanaswamy, K.; Scariah, K.J.; Nair, P.R.; Sastri, K.S.; Ang, H.G. Evaluation by various experimental approaches of the crosslink density of urethane networks based on hydroxyl-terminated polybutadiene. *J. Appl. Polym. Sci.* **2007**, *103*, 3129–3133. [[CrossRef](#)]
35. Venkataraman, S.; Alex, A.S.; Kumar, V.; Bandyopadhyay, G.G. Theoretical Evaluation of Crosslink Density of Chain Extended Polyurethane Networks Based on Hydroxyl Terminated Polybutadiene and Butanediol and Comparison with Experimental Data. *J. Energetic Mater.* **2018**, *36*, 38–47.
36. Jutrzenka Trzebiatowska, P.; Santamaria Echert, A.; Calvo Correias, T.; Eceiza, A.; Datta, J. The changes of crosslink density of polyurethanes synthesised with using recycled component. Chemical structure and mechanical properties investigations. *Prog. Org. Coat.* **2018**, *115*, 41–48. [[CrossRef](#)]
37. Ren, R.; Han, K.; Zhao, P.; Shi, J.; Zhao, L.; Gao, D.; Zhang, Z.; Yang, Z. Identification of asphalt fingerprints based on ATR-FTIR spectroscopy and principal component-linear discriminant analysis. *Constr. Build. Mater.* **2019**, *198*, 662–668. [[CrossRef](#)]
38. Xiao, D.; Le, T.T.G.; Doan, T.T.; Le, B.T. Coal identification based on a deep network and reflectance spectroscopy. *Spectrochim. Acta Part A Mol. Biomol. Spectrosc.* **2022**, *270*, 120859. [[CrossRef](#)]
39. Dong, Z. Study on Accelerated Polishing Test and the Regularity of Skid Resistance Degradation of Asphalt Pavement Material. Master's Thesis, Chang'an University, Xi'an, China, 2011.